

Performance Analysis of a Surface Permanent Magnet Motor

Abstract. In the paper the Finite Element Method (FEM) to analyse the performance characteristics of a surface permanent magnet motor is employed. The object of study is a permanent magnet motor with surface permanent magnets. Two rotor topologies are considered: surface-mounted (SM) and surface-inset (SI) magnets. Accepted constraints are to keep the same quality of the material and the same volume of permanent magnets. The research is consisted of FEM based numerical experiments that put in view properties of electromagnetic field, such as magnetic field distribution in the motor, magnetic flux per pole and components of the flux density in the air gap. In addition performance characteristics of back-emf, electromagnetic torque and cogging torque are determined and compared.

Streszczenie. W artykule został zaprezentowany algorytm oparty na Metodzie Elementów Skończonych (MES) do analizy charakterystyki działania silnika z powierzchniowym magnesem trwałym. Przeanalizowano dwa wirniki: z magnesem zamontowanym na powierzchni i magnesem wmontowanym. Ograniczenia polegają na utrzymaniu takiej samej jakości materiału i tej samej objętości magnesów. Badania polega na przeprowadzeniu, opartego na MES, eksperymentu, który analizuje własności pola elektromagnetycznego, takie jak rozkład pola magnetycznego w silniku, pole magnetyczne na biegun oraz składowe indukcji magnetycznej w szczeliny powietrznej. Wyznaczone również i porównano dla dwóch wirników charakterystykę siły elektromotorycznej, momentu elektromagnetycznego oraz momentu pulsacyjnego. (*Analiza działania silnika z powierzchniowym magnesem trwałym*).

Keywords: Permanent magnet motor, Surface mounted magnets, Surface inset magnets, Finite element analysis .

Słowa kluczowe: silnik z magnesem trwałym, magnes zamontowany powierzchniowo, magnes wmontowany powierzchniowo, metoda elementów skończonych

Introduction

In the recent years permanent magnet motors are replacing conventional electric motors, like induction and synchronous. It is mainly because of the fact that conventional motors are not suitable for applications that require "deep" speed regulation. Permanent magnet (PM) motors have the highest specific power density compared to other types of electric machines, which implies that they are lighter and occupy less space for a given power rating. In general, PM machines have a higher efficiency as result of the passive, PM-based, field excitation. Permanent magnet motors provide a high torque, smooth work and simple controllability. Even more, these motors have high torque to volume ratio, high torque to stator current ratio, and low inertia with very good dynamic response.

Several rotor structures of permanent magnet machines, each with specific strengths and weaknesses, are possible [1-3]. This variety depends on the shape of permanent magnets and their arrangement in the rotor [4]. Most of them use permanent magnets which are mounted *on* the rotor (exterior type motors), but they can be also placed *inside* the rotor core (interior type motors). In the paper we study an exterior type PM motor, with two possible positions of the permanent magnets: surface mounted (SM) magnets and surface inset (SI) magnets.

An accurate magnetic field analysis of the motor, which includes iron saturation, is performed by using the Finite Element Method [5]. Hereafter are calculated the radial and tangential components of the air gap flux density, induced back-emf, and by integrating weighted stress volume tensor of the rotor core, the cogging and electromagnetic torque characteristics are determined, too. The characteristics are presented on charts and analysed.

Surface Permanent Magnet Motor Topologies

In the surface type of permanent magnet motors, there are two possible placements of permanent magnets: permanent magnets are placed directly *on* the rotor surface – *surface mounted* (SM) magnets with non-uniform airgap, or they can be *surface inset* (SI) magnets placed *in* the rotor core, so that the outer surface of the rotor becomes cylindrical. These two rotor topologies are presented in Fig. 1 (a) and Fig. 1 (b), respectively. The magnetization in the

both magnet structures is radial. With permeability close to the air, from the "stator viewpoint" the permanent magnets appear as a large air gap.

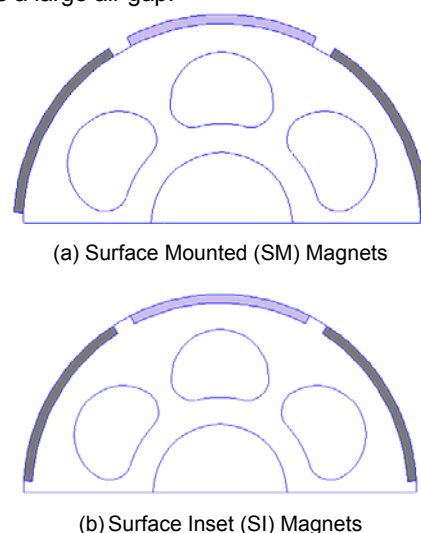


Fig. 1. Surface permanent magnet motor topologies

Studied Motor

There are few conventional PM motor configurations, but also other more novel concepts conceived in recent years, to improve motor performance. The position and relation of the rotor permanent magnets to the stator structure determine the properties and the shape of rotating magnetic field. The profile of the back-emf is one of the fundamental characteristics and it always matches with driving currents, being either trapezoidal or sinusoidal. Permanent magnet motors with trapezoidal back-emf are usually called brushless DC permanent magnet motors (BLDCPM), while those with sinusoidal back-emf are referred to as PM synchronous motors (PMSM).

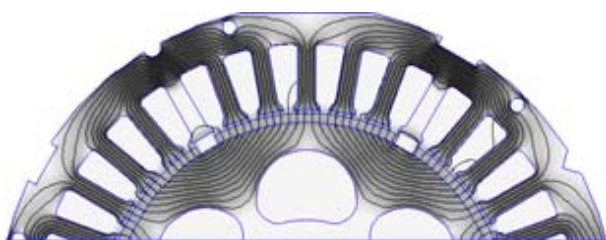
The studied machine is a BLDCPM type, with surface permanent magnets of the rotor. This sort of motor is simple in construction. The three-stage stator winding is placed in 36 slots and is supplied by rectangular waves of currents. There are 6 permanent magnets placed in two ways on the

rotor, as shown in Fig. 1 (a) and (b), for a half of the rotor cross-section. The magnets are made of SmCo material; they are radially magnetised and built with 9 segments along the pole arc. The operating magnetic flux density in the air-gap is nearly the same as of magnets, so the air-gap flux densities are close to the remanent flux density of the permanent magnets i.e. 1.0 – 1.2 T.

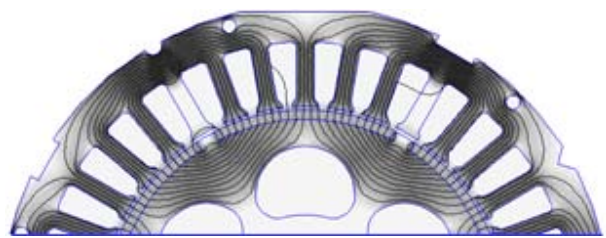
FEM Computations

Among several approaches [6-8], two-dimensional Finite Element Method is employed for prediction the performance characteristics of the studied surface permanent magnet (SPM) motor. The mesh of finite elements, is consisted of more than 122,000 nodes and 243,000 elements; it is spread over the full cross section of the motor.

The calculations start with no-load, i.e. without current in the armature windings, when magnetic field is produced only by excitation of permanent magnets. A part of magnetic flux distribution, for the two layouts of permanent magnets, is shown in Fig. 2 (a) and (b).



(a) Surface Mounted (SM) Magnets



(b) Surface Inset (SI) Magnets

Fig. 2. Magnetic field at no-load $I = 0$ A; initial position $\theta = 0^\circ$

The study presented in this paper is mainly a simulation one. Usually, there are different FEM ways that can be employed in numerical simulations and they depend on the state of the analysed system, i.e. steady state or transient operation. We intend to focus on the properties of the magnetic field created by permanent magnets; hence the magnetostatic analysis is relevant. It has to be pointed out that this FEM approach catches a given moment of the motor operation; thus, rotation, speed or voltage/current variations are not considered.

Magnetic flux per pole and its shape is an important parameter that determines the performance of the surface permanent magnet motor. Since the presented research has a comparative character, two placements of permanent magnets in the rotor described before, are considered: surface mounted and surface inset. Using a series of FEM field calculations, the comparative characteristics $\Phi_p=f(\theta)$ at no-load is determined and presented in Fig. 3.

From the following figure it is evident that there is no significant difference between the motor characteristics at surface and inset placement of the permanent magnets. As an example can serve the maximum value of magnetic flux per pole, which is for SM magnets 2.31 mVs, while for SI magnets it is 2.24 mVs, that gives ~3.1% difference; at the

same time, the profiles of their characteristics $\Phi_p=f(\theta)$ are almost identical, resembling the sinusoidal shape.

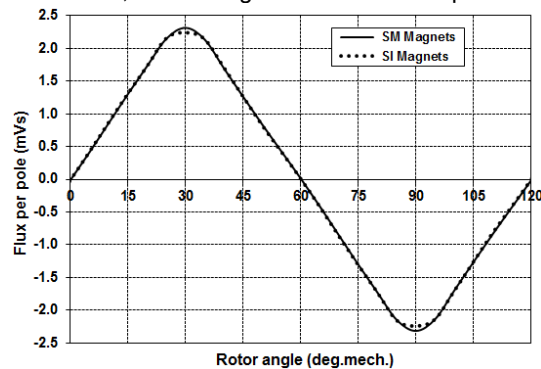


Fig. 3. Comparative characteristics of the magnetic flux per pole $\Phi_p=f(\theta)$ at no-load

The FEM computations continue at loading conditions. In Fig. 4 (a) and (b) are presented magnetic flux density colour maps and flux lines at rated current $I_n = 18$ A, when the rotor position is $\theta = 30^\circ$ mech. = 90° el., for the analysed layouts of the permanent magnets: surface mounted and surface inset, respectively.



(a) Surface Mounted (SM) Magnets



(b) Surface Inset (SI) Magnets

Fig. 4. Magnetic field distribution at rated load $I_n = 18$ A and for rotor position $\theta = 30^\circ$ mech.

Based on the series of numerical experiments by using FEM, for two defined rotor structures, the performance characteristics at loading operation of the studied motor are computed, presented on charts and analysed. The results are shown comparatively, where solid line is related to SM magnets, while dotted line refers to SI magnets.

The electromagnetic characteristics, when the magnetic field is excited by interaction of permanent magnets and rated armature current, are determined; profiles of radial and tangential components of magnetic flux density along the mid-line of the air-gap, as well as the magnetic flux per pole are presented in the next figures.

The distribution of the normal component for the air-gap magnetic flux density at rated load is presented in Fig. 5, while the tangential component is given in Fig. 6.

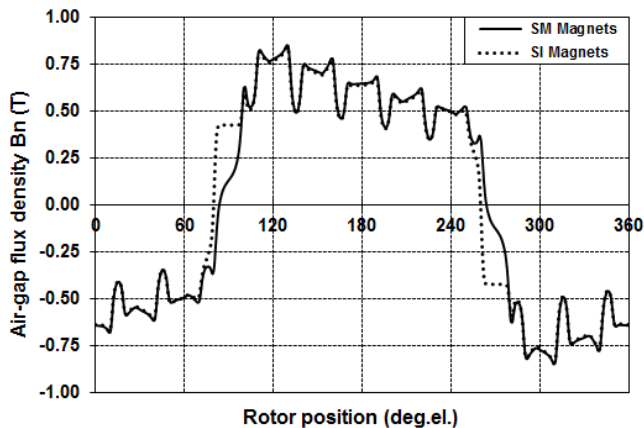


Fig. 5. Comparative characteristics of the radial component distribution for the air-gap magnetic flux density at rated load

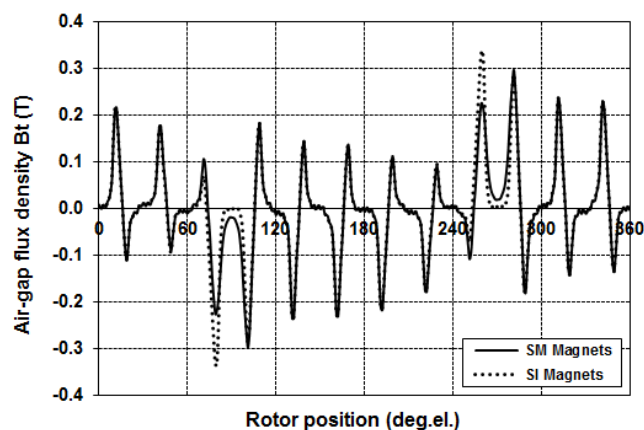


Fig. 6. Comparative characteristics of the tangential component distribution for the air-gap magnetic flux density at rated load

From the review of the magnetic field properties, shown in the previous figures, two motor topologies exhibit similar features. A more significant disagreement usually will appear along the q -axis. i.e. $\theta=30^0$ mech. $=90^0$ el.

Table 1 Magnetic field properties of SPM motor for two layouts of permanent magnets

Description	Unit	No-load $I = 0$ A; Initial position $\theta = 0^0$ mech.		Rated load $I_n = 18$ A; Initial position $\theta = 0^0$ mech.		Rated load $I_n = 18$ A; Position $\theta = 30^0$ mech.	
		SM magnets	SI magnets	SM magnets	SI magnets	SM magnets	SI magnets
Magnetic vector potential A_{max}	V/s	0.01334	0.01356	0.01496	0.01518	0.01330	0.01441
Magnetic flux per pole Φ_p	mVs	2.31405	2.24051	2.59865	2.52863	0.38279	0.52613
Magnetic flux density B_m	T	0.55052	0.53303	0.61823	0.60157	0.09107	0.12517

A selection of several typical results, extracted from the FEM calculations, at no-load and at rated load operation, are presented in Table 1; SM refers to surface mounted, while SI is related to surface inset magnets.

The calculations of torques are based on numerical integration of the volume Weighted Stress Tensor affecting the rotor. The use of volume integral greatly simplifies the

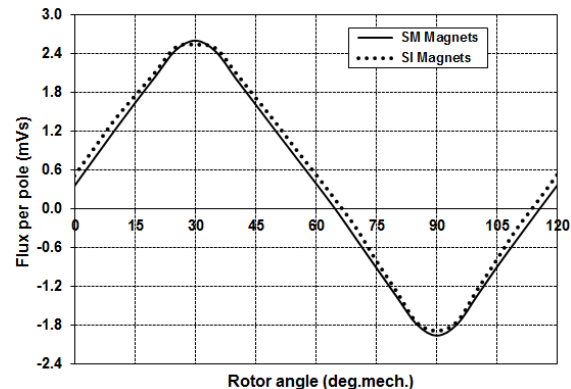


Fig. 7. Flux characteristics $\Phi_p=f(\theta)$ at rated load $I_n=18$ A

In Fig. 7 are presented comparative characteristics of the magnetic flux per pole $\Phi_p=f(\theta)$ at rated current.

Analysis of Results

To complete the performance analysis of the surface permanent magnet motor, it is determined the shape of induced back-emf characteristic E , by using the expression:

$$(1) \quad E = W_c \cdot \frac{\Delta\phi}{\Delta t}$$

where: W_c is the number of turns per coil of the armature winding; ϕ (Vs) is the air-gap flux excited by the permanent magnets, and t is time (s).

For motor speed of 1000 rpm (i.e. for frequency 50 Hz), the characteristic $E(\theta)$ is calculated and is depicted in Fig. 8. Analysing the chart, as one can expect, its shape is (almost) trapezoidal. The appearance of a flat part of the characteristics is influenced by the stator teeth

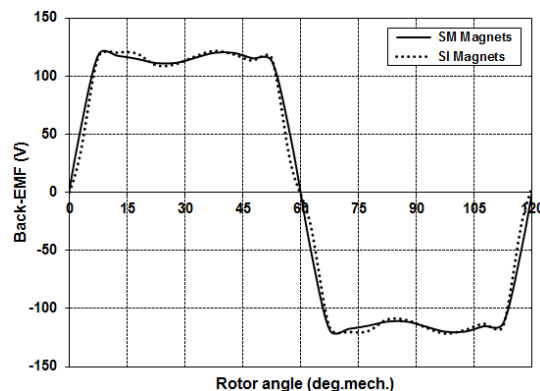


Fig. 8. Induced back-emf characteristics

numerical computation of forces and torques, as compared to evaluating them via the stress tensor line integral, or to differentiation of magnetic coenergy of the air gap region.

No particular "art" is required in getting good results for torque; however, it should be stressed that results tend to be more accurate with finer meshing in the region where the torque is to be determined. The only limitation for the

application of the method is that the regions upon which the torque is being computed must be entirely surrounded by air and/or abutting any boundary.

From the FE postprocessing results, when the magnetic field is energized by the permanent magnets only, first, the cogging torque is computed; the respective comparative profiles of the cogging torque are presented in Fig. 9.

In the next step, rated current is injected in the armature (stator) windings, and the static electromagnetic torque is determined. For initial position and 0° mech. is defined the position at which rotor and stator magnetic field are aligned, i.e. along the d-axis. The respective comparative charts, for analysed permanent magnets layouts are shown in Fig. 10.

As one could expect, both diagrams are showing bigger disagreement along q-axis, where an evident discrepancy of the rotor topology appears.

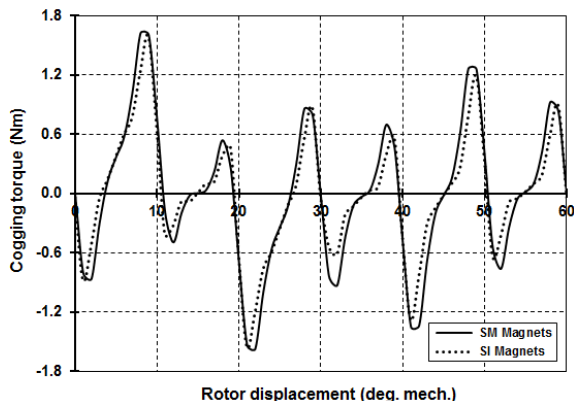


Fig. 9 Cogging torque profiles

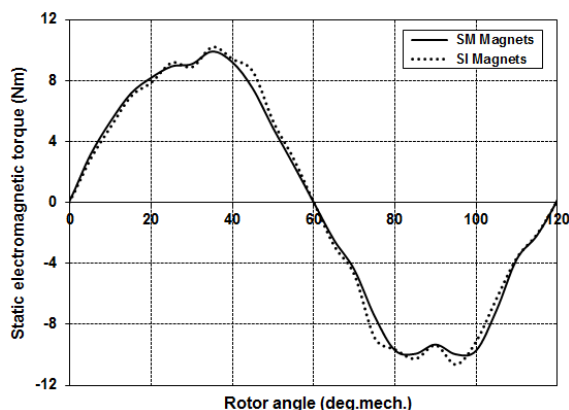


Fig. 10 Static torque characteristics at rated load

Conclusions

In the present paper, the object of study is a permanent magnet motor with surface permanent magnets. Two rotor topologies are considered: surface-mounted (SM) and surface-inset (SI) magnets. Based on FEM numerical simulations, the performance characteristics of the motor are determined and analysed. The 2D magnetostatic FEM

computational results are used as powerful numerical tool for performance analyses, enabling the visibility of the magnetic characteristics features.

Accepted constraints are to keep the same quality of the material and the same volume of permanent magnets. The emphasis is put on the properties of electromagnetic field, such as magnetic field distribution in the motor domain, the magnetic flux per pole, as well as components of the flux density in the air gap.

In addition the profile of back-emf, cogging torque and static electromagnetic torque are calculated and compared.

The next task will be to analyse the losses in permanent magnets. By using the time-stepping method the calculation of iron loss, overall losses and efficiency of the SPM motor, could also be of interest.

This work could serve as a good guide.

Authors: The authors are with Ss. Cyril and Methodius University, Faculty of Electrical Engineering and Information Technologies, Rugjer Boskovic bb, P. O. Box 574, MK-1000 Skopje, Macedonia.

Prof. Dr. Lidija Petkovska, e-mail: lidijap@feit.ukim.edu.mk

REFERENCES

- [1] Finken, T., Hombitzer, M., Hameyer, K. (2010) Study and Comparison of several Permanent-Magnet excited Rotor Types regarding their Applicability in Electric Vehicles, in *Proceedings of E-mobility – Electrical Power Train Conference*, on CD, pp. 1-7, Leipzig, Germany.
- [2] Arora, A. S., Singh, G. (2015) Review of Design and Performance of Permanent Magnet Synchronous Motor, *International Journal of Industrial Electronics and Electrical Engineering – IJIEEE*, Vol. 3, No. 10, pp. 20-28.
- [3] Jabbar, M. A., Khambadkone, A. M., Qinghua, L. (2011) Design And Analysis Of Exterior And Interior Type High-Speed Permanent Magnet Motors, in *Proceedings of Australian Universities Power Engineering Conference (AUPEC'2011)*, pp. 472-476.
- [4] Pellegrino G., Vagati A., Guglielmi P., Boazzo B. (2012). Performance comparison between Surface Mounted and Interior PM motor drives for Electric Vehicle application, in *IEEE Transactions on Industrial Electronics*, Vol. 59 No. 2, pp. 803-811.
- [5] Vimalakeerthy, D., Kanagaraj, N., Sanavullah, M. Y. (2013) Novel Design of Permanent Magnet Synchronous Reluctance Motor using Finite Element Method, *International Journal of Engineering Science and Innovative Technology (IJESIT)*, Vol. 2, Issue 1, pp. 37-45.
- [6] Boughrara, K., Zarko, D., Ibtouen, R., Touhami, O., Rezzoug, A. (2009) Magnetic Field Analysis of Inset and Surface-Mounted Permanent-Magnet Synchronous Motors Using Schwarz-Christoffel Transformation, *IEEE Transactions on Magnetics*, Vol. 45, No. 8, pp. 3166-3178.
- [7] Lubin, T., Mezani, S., Rezoug, A. (2012) 2D Analytical Calculation of Magnetic Field and Electromagnetic Torque for Surface-Inset Permanent-Magnet Motors, *IEEE Transactions on Magnetics*, Vol. 48, No. 6, pp. 2080-2091.
- [8] Mohammadi, S., Mirsalim, M., Vaez-Zadeh, S. (2014), Nonlinear Modeling of Eddy-Current Couplers, *IEEE Transactions on Energy Conversion*, Vol. 29, No. 1, pp. 224-231.